AIAA JOURNAL
Vol. 30, No. 8, August 1992

Layer-Wise Shell Theory for Postbuckling of Laminated Circular Cylindrical Shells

J. N. Reddy* and M. Savoia†
Virginia Polytechnic Institute and State University, Blacksburg, Virginia 24061

The layer-wise shell theory of Reddy is used to study the postbuckling response of circular cylindrical shells. The Rayleigh-Ritz method is used to solve the equations by assuming a double Fourier expansion of the displacements with trigonometric coordinate functions. Numerical results for postbuckling response of axially compressed multilayer cylinders with simply supported edge conditions are presented for different values of shell imperfections.

I. Introduction

THE problem of buckling and postbuckling analyses of axially loaded cylindrical shells has attracted an enormous research interest, and it has been the subject of many different theoretical approaches. Nevertheless, questions yet remain about a complete understanding of all of the details of the phenomena involved.[1-5]

In addition, in recent years the increasing need for lightweight structural elements has led to the use of fiber-reinforced multilayered structures. In this context, Koiter-type b-factor analyses[6] have shown that optimization of the axial buckling load with respect to the laminate properties may cause a large increase in imperfection sensitivity.[7] Pandey and Sherbourne[8] remarked that the criteria for optimality of the load capability and reduced imperfection sensitivity are often competing factors.

Thin elastic shells subjected to predominantly compressive membrane stress states show a tendency to buckle explosively and the loss of stability occurs at loads far below those predicted by a linear eigenvalue analysis. To capture this phenomenon, an imperfection sensitivity analysis is usually performed by analyzing the initial postbuckling response, within the context of Koiter's general theory. Even though this analysis usually indicates an unstable bifurcation, the possibility does exist that a higher load than the bifurcation point can be supported before the total collapse occurs. Moreover, advanced postbuckling analyses[2,9] showed that for large imperfection amplitudes the bifurcation becomes stable so that higher loads can be sustained.

In the past, imperfection sensitivity studies as well as full nonlinear analyses of isotropic and multilayered cylindrical shells were often performed disregarding the effects of end conditions by assuming that the cylinder is infinitely long. These simplified studies can help to understand the extremely complex behavior of thin isotropic[10-13] and composite[14,15] circular cylinders in compression. Such studies also help to outline some perplexing phenomena.[16] However, a systematic experimental investigation[17,18] of cylinders of different length revealed the strong influence of the cylinder length on the buckling behavior, namely, on the wave length into which the shell buckles.[19-21]

With few exceptions,[22,23] postbuckling analyses of multilayered cylindrical shells have been performed only by the classical laminate theory, that is, the theory based on the Kirchhoff hypothesis. It is well known that this theory is adequate for isotropic shells when the thickness-radius ratio is very small. When fiber-reinforced composites are considered, the transverse shear strains must be taken into account since the ratio between the layer extensional modulus along the fiber direction and the shear moduli is usually very large, even 50 times larger than for isotropic materials.

In addition, when layers with very dissimilar material properties are bonded together, the continuity of the stress vector at the layer interface requires discontinuity of the strain components and, consequently, displacements with discontinuous derivatives in the thickness direction at the interlaminae.[24,25]

In the present study, the layer-wise shell theory of Reddy[26-28] is used for the postbuckling analysis of laminated cylindrical shells subjected to compressive axial loads. There exists several other layer-wise theories, as reviewed by Reddy.[24] To distinguish the layer-wise theory used here from those proposed by others, the present layer-wise theory is called the layer-wise theory of Reddy (see also Ref. 29). This theory assures an accurate description of the three-dimensional displacement field by expanding it as a linear combination of layer-wise thickness approximation functions and unknown functions defined over the mean surface of the shell.

The nonlinear strain-displacement relations for shells with small geometric imperfections are assumed, based on the Mushtari-Vlasov-Donnell kinematic approximation of small strains and negligible small rotations. Despite their simplicity, these equations yield very accurate results in terms of buckling and maximum loads for shell with Batdorf curvature parameters $Z < 10{,}000$ (for isotropic shells).[30,31]

The governing differential equations of the layer-wise shell theory are obtained by the application of the principle of virtual displacements. The displacements are represented in the surface of the shell by means of a double trigonometric expansion, and the Rayleigh-Ritz method is used to obtain the nonlinear set of algebraic equations.

A linearized (eigenvalue) buckling analysis[28] was previously performed using the layer-wise theory. The development is extended here to postbuckling analysis. It is shown that thin isotropic shells require a large number of terms in the expansion to perform a multimode analysis,[32,33] whereas orthotropic and multilayered cylinders require only few terms. Numerical results are presented for the postbuckling response of axially compressed multilayered cylinders for different values of shell imperfection. Maximum loads equal to 40–60% of the linear buckling loads are obtained in the examples presented herein.

II. Governing Equations

A. Displacement and Strain Fields

Consider a laminated circular cylindrical shell of total thickness h, mean radius R, and length L. The laminate is made of

Received Sept. 17, 1991; revision received Jan. 27, 1992; accepted for publication Jan. 27, 1992.

*Clifton C. Garvin Professor, Department of Engineering Science and Mechanics; currently, Oscar S. Waytt Chair, Department of Mechanical Engineering, Texas A&M University, College Station, TX 77843.

†Visiting Scientist; Assistant Professor, University of Bologna, Italy.

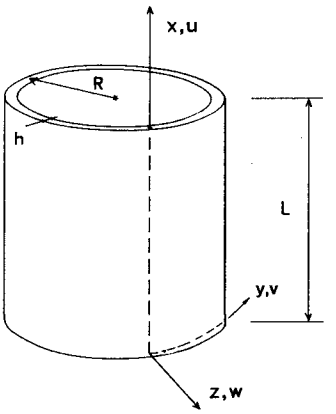

Fig. 1 Geometry, coordinate system, and notation for displacements of a circular cylindrical shell.

N cross-ply orthotropic layers. The cylinder is simply supported on its edges. A local coordinate system (x, y, z) is used (see Fig. 1), in which x and y are in the axial and circumferential directions, and z is in the direction of the outward normal to the middle surface; the corresponding displacements are designated by u, v, and w. In addition, $\hat{w}$ denotes the radial deviation (i.e., geometric imperfection) of the shell from the perfectly cylindrical shape.

In order to assure an accurate description of the displacement components, the layer-wise theory of Reddy is used. In the layer-wise theory, the displacement is expanded as follows.[28]

$$\begin{aligned} u(x,y,z) &= \sum_{i=1}^{N+1} u_i(x,y)\Phi^i(z) = u_i\Phi^i \\ v(x,y,z) &= \sum_{i=1}^{N+1} v_i(x,y)\Phi^i(z) = v_i\Phi^i \\ w(x,y,z) &= \sum_{i=1}^{N+1} w_i(x,y)\Phi^i(z) = w_i\Phi^i \\ \hat{w}(x,y,z) &= \sum_{i=1}^{N+1} \hat{w}_i(x,y)\Phi^i(z) = \hat{w}_i\phi^i \end{aligned} \tag{1}$$

where u_i, v_i, and w_i are the unknown functions to be determined, and $\hat{w}_i$ are assigned geometric imperfections. In Eqs. (1), summation on repeated indices is assumed. The Φ^i are assumed to be linear approximation functions with local support that assume value equal to 1 at the ith interface and 0 at the jth interface, $i \neq j$:

$$\Phi^i = \begin{cases} \psi_2^{i-1} \equiv \dfrac{z - z_{i-1}}{h_{i-1}}, & z_{i-1} \le z \le z_i \\ \psi_1^i \equiv \dfrac{z_i - z}{h_i}, & z_i \le z \le z_{i+1} \end{cases} \tag{2}$$

Considering a small shell thickness when compared with the radius of curvature R (i.e., shallow shell theory) and taking into account the nonlinear strains due to large radial displacements, the following nonlinear Mushtari-Vlasov-Donnell strain-displacement relations[34] are obtained:

$$\epsilon_1 \equiv \epsilon_{11} = \frac{\partial u}{\partial x} + \frac{\partial w}{\partial x}\left(\frac{1}{2}\frac{\partial w}{\partial x} + \frac{\partial \hat{w}}{\partial x}\right)$$

$$\epsilon_2 \equiv \epsilon_{22} = \frac{\partial v}{\partial y} + \frac{w}{R} + \frac{\partial w}{\partial y}\left(\frac{1}{2}\frac{\partial w}{\partial y} + \frac{\partial \hat{w}}{\partial y}\right)$$

$$\epsilon_3 \equiv \epsilon_{33} = \frac{\partial w}{\partial z}, \quad \epsilon_4 \equiv 2\epsilon_{23} = \frac{\partial v}{\partial z} + \frac{\partial w}{\partial y} - \frac{v}{R}$$

$$\epsilon_5 \equiv 2\epsilon_{13} = \frac{\partial u}{\partial z} + \frac{\partial w}{\partial x}$$

$$\epsilon_6 \equiv 2\epsilon_{12} = \frac{\partial u}{\partial y} + \frac{\partial v}{\partial x} + \frac{\partial w}{\partial x}\left(\frac{1}{2}\frac{\partial w}{\partial y} + \frac{\partial \hat{w}}{\partial y}\right) + \frac{\partial w}{\partial y}\left(\frac{1}{2}\frac{\partial w}{\partial x} + \frac{\partial \hat{w}}{\partial x}\right) \tag{3}$$

Here, the single subscript notation of strains is introduced. Similar notation will be used for stress components.

B. Virtual Work Statement

Suppose that the circular cylindrical shell is subjected to axial load distribution q at the ends and internal and external pressure distributions p_b and p_t. The minimum total potential energy principle is used to derive the governing equations. The minimum total potential energy principle states that $\delta\Pi = 0$, where $\delta\Pi$ is the first variation of the total potential energy,

$$\begin{aligned} \delta\Pi = &\int_0^L\int_0^{2\pi R}\int_{-h/2}^{h/2} \sigma_i\delta\epsilon_i \, dz \, dy \, dx - \int_0^{2\pi R}\int_{-h/2}^{h/2} [q(y,z)\delta u|_{x=0} \\ &+ q(y,z)\delta u|_{x=L}] \, dz \, dy - \int_0^L\int_0^{2\pi R} [p_b(x,y)\delta w|_{z=-h/2} \\ &+ p_t(x,y)\delta w|_{z=h/2}] \, dy \, dx \end{aligned} \tag{4}$$

Substituting the strain-displacement relations (3) and the displacement representation (1) in Eq. (4), and integrating through the thickness we obtain

$$\begin{aligned} &\int_0^L\int_0^{2\pi R}\left\{M_1^i\frac{\partial\delta u_i}{\partial x} + M_1^{ij}\frac{\partial\delta w_i}{\partial x}\left(\frac{\partial w_j}{\partial x} + \frac{\partial\hat{w}_j}{\partial x}\right)\right. \\ &+ M_2^i\left(\frac{\partial\delta v_i}{\partial y} + \frac{1}{R}\delta w_i\right) + M_2^{ij}\frac{\partial\delta w_i}{\partial y}\left(\frac{\partial w_j}{\partial y} + \frac{\partial\hat{w}_j}{\partial y}\right) \\ &+ M_6^i\left(\frac{\partial\delta u_i}{\partial y} + \frac{\partial\delta v_i}{\partial x}\right) + M_6^{ij}\left[\frac{\partial\delta w_i}{\partial x}\left(\frac{\partial w_j}{\partial y} + \frac{\partial\hat{w}_j}{\partial y}\right)\right. \\ &\left.\left. + \frac{\partial\delta w_i}{\partial y}\left(\frac{\partial w_j}{\partial x} + \frac{\partial\hat{w}_j}{\partial x}\right)\right] + Q_3^i\delta w_i + Q_4^i\delta v_i \right. \\ &\left. + K_4^i\left(-\frac{1}{R}\delta v_i + \frac{\partial\delta w_i}{\partial y}\right) + Q_5^i\delta u_i + K_5^i\frac{\partial\delta w_i}{\partial x}\right\} dx \, dy \\ &- \int_0^{2\pi R} T_i(q\cdot\delta u_i|_{x=0} + q\cdot\delta u_i|_{x=L}) \, dy \\ &- \int_0^L\int_0^{2\pi R} [p_b(x,y)\delta w_1 + p_t(x,y)\delta w_{N+1}] \, dy \, dx = 0 \end{aligned} \tag{5}$$

where the axial load q is assumed constant through the thickness, and the laminate resultants M_α^i, M_α^{ij}, Q_α^i, K_α^i, and T_i are defined as follows:

$$\begin{aligned} M_\alpha^i &= \int_{-h/2}^{h/2} \sigma_\alpha\Phi^i \, dz, \quad M_\alpha^{ij} = \int_{-h/2}^{h/2} \sigma_\alpha\Phi^i\Phi^j \, dz \quad (\alpha = 1,2,6) \\ Q_\alpha^i &= \int_{-h/2}^{h/2} \sigma_\alpha\frac{d\Phi^i}{dz} \, dz (\alpha = 3,4,5) \\ K_\alpha^i &= \int_{-h/2}^{h/2} \sigma_\alpha\Phi^i \, dz \quad (\alpha = 4,5) \end{aligned} \tag{6}$$

$$T_i = \int_{-h/2}^{h/2} \Phi^i \, dz = \begin{cases} \dfrac{t_i + t_{i+1}}{2} & 2 \le i \le N \\ t_{1/2} & i = 1 \\ t_{N-2} & i = N+1 \end{cases}$$

We assume that the laminated cylindrical shell is made of orthotropic layers with elastic symmetry with respect to the

dent with the axial and circumferential directions x and y (cross-ply lamination scheme). Then the layer constitutive equations can be written as,

$$\sigma_i = C_{ij}\epsilon_j \quad (i,j = 1, 2, 3)$$
$$\sigma_i = C_{ii}\epsilon_i \quad (i = 4, 5, 6; \text{ no sum on } i) \tag{7}$$

where C_{ij} are elastic coefficients of the layer, and single subscript notation for stresses is used:

$$\sigma_1 = \sigma_{11}, \quad \sigma_2 = \sigma_{22}, \quad \sigma_3 = \sigma_{33}$$
$$\sigma_4 = \sigma_{23}, \quad \sigma_5 = \sigma_{13}, \quad \sigma_6 = \sigma_{12} \tag{8}$$

Using Eqs. (7), the stress resultants in Eqs. (6) can be expressed in terms of the generalized displacements.

C. Total Potential Energy in Terms of Displacements

Consider a cylinder subjected to constant axial load q_0 and constant external and internal pressure distributions p_t and p_b. By substituting the laminate resultants (6) in terms of displacements into the statement (5), collecting terms involving the variations of functions (u_i, v_i, w_i) separately, the following governing equations are obtained:

δu_i:

$$\int_0^L\int_0^{2\pi R}\left(\frac{\partial\delta u_i}{\partial x}\left[D_{11}^{ij}\frac{\partial u_j}{\partial x} + D_{11}^{ijk}\frac{\partial w_j}{\partial x}\left(\frac{1}{2}\frac{\partial w_k}{\partial x} + \frac{\partial\hat{w}_k}{\partial x}\right) + D_{12}^{ij}\left(\frac{\partial v_j}{\partial y} + \frac{w_j}{R}\right) + D_{12}^{ijk}\frac{\partial w_j}{\partial y}\left(\frac{1}{2}\frac{\partial w_k}{\partial y} + \frac{\partial\hat{w}_k}{\partial y}\right) + \bar{D}_{13}^{ij}w_j\right] + \frac{\partial\delta u_i}{\partial y}\left\{D_{66}^{ij}\left(\frac{\partial u_j}{\partial y} + \frac{\partial v_j}{\partial x}\right) + D_{66}^{ijk}\left[\frac{\partial w_j}{\partial x}\left(\frac{1}{2}\frac{\partial w_k}{\partial y} + \frac{\partial\hat{w}_k}{\partial y}\right) + \frac{\partial w_j}{\partial y}\left(\frac{1}{2}\frac{\partial w_k}{\partial x} + \frac{\partial\hat{w}_k}{\partial x}\right)\right]\right\} + \delta u_i\left(\bar{D}_{55}^{ij}u_j + D_{55}^{ji}\frac{\partial w_j}{\partial x}\right)\right)dy\,dx - q_0 2\pi R T_i\left(\delta u_i\Big|_{x=0} + \delta u_i\Big|_{x=L}\right) = 0 \tag{9a}$$

δv_i:

$$\int_0^L\int_0^{2\pi R}\left(\frac{\partial\delta v_i}{\partial y}\left[D_{12}^{ij}\frac{\partial u_j}{\partial x} + D_{12}^{ijk}\frac{\partial w_j}{\partial x}\left(\frac{1}{2}\frac{\partial w_k}{\partial x} + \frac{\partial\hat{w}_k}{\partial x}\right) + D_{22}^{ij}\left(\frac{\partial v_j}{\partial y} + \frac{w_j}{R}\right) + D_{22}^{ijk}\frac{\partial w_j}{\partial y}\left(\frac{1}{2}\frac{\partial w_k}{\partial y} + \frac{\partial\hat{w}_k}{\partial y}\right) + \bar{D}_{23}^{ij}w_j\right] + \frac{\partial\delta v_i}{\partial x}\left\{D_{66}^{ij}\left(\frac{\partial u_j}{\partial y} + \frac{\partial v_j}{\partial x}\right) + D_{66}^{ijk}\left[\frac{\partial w_j}{\partial x}\left(\frac{1}{2}\frac{\partial w_k}{\partial y} + \frac{\partial\hat{w}_k}{\partial y}\right) + \frac{\partial w_j}{\partial y}\left(\frac{1}{2}\frac{\partial w_k}{\partial x} + \frac{\partial\hat{w}_k}{\partial x}\right)\right]\right\} + \delta v_i\left[\left(\bar{D}_{44}^{ij} - \frac{1}{R}\bar{D}_{44}^{ij}\right)v_j + \left(\bar{D}_{44}^{ji} - \frac{1}{R}D_{44}^{ji}\right)\left(\frac{\partial w_j}{\partial y} - \frac{v_j}{R}\right)\right]\right) = 0 \tag{9b}$$

δw_i:

$$\int_0^L\int_0^{2\pi R}\left\{\frac{1}{R}\delta w_i\left[D_{12}^{ij}\frac{\partial u_j}{\partial x} + D_{12}^{ijk}\frac{\partial w_j}{\partial x}\left(\frac{1}{2}\frac{\partial w_k}{\partial x} + \frac{\partial\hat{w}_k}{\partial x}\right) + D_{22}^{ij}\left(\frac{\partial v_j}{\partial y} + \frac{w_j}{R}\right) + D_{22}^{ijk}\frac{\partial w_j}{\partial y}\left(\frac{1}{2}\frac{\partial w_k}{\partial y} + \frac{\partial\hat{w}_k}{\partial y}\right) + \bar{D}_{23}^{ij}w_j\right] + \delta w_i\left[\bar{D}_{13}^{ji}\frac{\partial u_j}{\partial x} + \bar{D}_{13}^{jki}\frac{\partial w_j}{\partial x}\left(\frac{1}{2}\frac{\partial w_k}{\partial x} + \frac{\partial\hat{w}_k}{\partial x}\right) + \bar{D}_{23}^{ji}\left(\frac{\partial v_j}{\partial y} + \frac{w_j}{R}\right) + \bar{D}_{23}^{jki}\frac{\partial w_j}{\partial y}\left(\frac{1}{2}\frac{\partial w_k}{\partial x} + \frac{\partial\hat{w}_k}{\partial y}\right) + \bar{D}_{33}^{ij}w_j\right] + \frac{\partial\delta w_i}{\partial x}\times\left[\bar{D}_{55}^{ij}u_j + D_{55}^{ji}\frac{\partial w_j}{\partial x}\right] + \frac{\partial\delta w_i}{\partial y}\left[\bar{D}_{44}^{ij}v_j + D_{44}^{ji}\left(\frac{\partial w_j}{\partial y} - \frac{v_j}{R}\right)\right] + \frac{\partial\delta w_i}{\partial x}\left(\frac{\partial w_j}{\partial x} + \frac{\partial\hat{w}_j}{\partial x}\right)\left[D_{11}^{ijk}\frac{\partial u_k}{\partial x} + D_{11}^{ijkl}\frac{\partial w_k}{\partial x}\left(\frac{1}{2}\frac{\partial w_l}{\partial x} + \frac{\partial\hat{w}_l}{\partial x}\right) + D_{12}^{ijk}\left(\frac{\partial v_k}{\partial y} + \frac{w_k}{R}\right) + D_{12}^{ijkl}\frac{\partial w_k}{\partial y}\left(\frac{1}{2}\frac{\partial w_l}{\partial y} + \frac{\partial\hat{w}_l}{\partial y}\right) + \bar{D}_{13}^{ijk}w_k\right] + \frac{\partial\delta w_i}{\partial y}\left(\frac{\partial w_j}{\partial y} + \frac{\partial\hat{w}_j}{\partial y}\right)\left[D_{12}^{ijk}\frac{\partial u_k}{\partial x} + D_{12}^{ijkl}\frac{\partial w_k}{\partial x}\left(\frac{1}{2}\frac{\partial w_l}{\partial x} + \frac{\partial\hat{w}_l}{\partial x}\right) + D_{22}^{ijk}\left(\frac{\partial v_k}{\partial y} + \frac{w_k}{R}\right) + D_{22}^{ijkl}\frac{\partial w_k}{\partial y}\left(\frac{1}{2}\frac{\partial w_l}{\partial y} + \frac{\partial\hat{w}_l}{\partial y}\right) + \bar{D}_{23}^{ijk}w_k\right] + \left[\frac{\partial\delta w_l}{\partial x}\left(\frac{\partial w_j}{\partial y} + \frac{\partial\hat{w}_j}{\partial y}\right) + \frac{\partial\delta w_i}{\partial y}\left(\frac{\partial w_j}{\partial x} + \frac{\partial\hat{w}_j}{\partial x}\right)\right]\left\{D_{66}^{ijk}\left(\frac{\partial u_k}{\partial y} + \frac{\partial v_k}{\partial x}\right) + D_{66}^{ijkl}\left[\frac{\partial w_k}{\partial x}\left(\frac{1}{2}\frac{\partial w_l}{\partial y} + \frac{\partial\hat{w}_l}{\partial y}\right) + \frac{\partial w_k}{\partial y}\left(\frac{1}{2}\frac{\partial w_l}{\partial x} + \frac{\partial\hat{w}_l}{\partial x}\right)\right]\right\}dy\,dx - 2\pi RL\left[p_b\delta w_i\delta_{(1)}^{(i)} + p_t\delta w_i\delta_{N+1}^{(i)}\right] = 0 \tag{9c}$$

where $\delta_{(j)}^{(i)}$ is the Kronecker delta and the laminate stiffnesses appearing in Eqs. (9) are defined as

$$D_{\alpha\beta}^{ij} = \int_{-h/2}^{h/2} C_{\alpha\beta}\Phi^i\Phi^j\,dz, \qquad D_{\alpha\beta}^{ijk} = \int_{-h/2}^{h/2} C_{\alpha\beta}\Phi^i\Phi^j\Phi^k\,dz$$
$$\bar{D}_{\alpha\beta}^{ij} = \int_{-h/2}^{h/2} C_{\alpha\beta}\Phi^i\frac{d\Phi^j}{dz}dz, \qquad D_{\alpha\beta}^{ijkl} = \int_{-h/2}^{h/2} C_{\alpha\beta}\Phi^i\Phi^j\Phi^k\Phi^l\,dz \tag{10}$$
$$\bar{D}_{\alpha 3}^{ijk} = \int_{-h/2}^{h/2} C_{\alpha 3}\Phi^i\Phi^j\frac{d\Phi^k}{dz}dz, \qquad \bar{\bar{D}}_{\alpha\beta}^{ij} = \int_{-h/2}^{h/2} C_{\alpha\beta}\frac{d\Phi^i}{dz}\frac{d\Phi^j}{dz}dz$$

where $i,j,k,l = 1, 2, \ldots, N+1$. The explicit form of these coefficients is given in Appendix 1 of Reddy and Savoia.[35]

III. Rayleigh-Ritz Solution

In order to solve system (9), the Rayleigh-Ritz method is used. The unknown displacements are expressed in terms of a double trigonometric series. For simply supported boundary conditions, the following solution form, which satisfies the boundary conditions $u_i = 0$ (at $x = L/2$), $v_i = 0$, $w_i = 0$, and $\hat{w}_i = 0$ (at $x = 0,L$) is used:

$$u_i = U_i^{mn}\cos\alpha_m x\cos\beta_n y$$
$$(m = 1, \ldots, M; n = 0, \ldots, N)$$
$$v_i = V_i^{mn}\sin\alpha_m x\sin\beta_n y \tag{11}$$
$$(m = 1, \ldots, M; n = 1, \ldots, N)$$
$$w_i = W_i^{mn}\sin\alpha_m x\cos\beta_n y$$
$$(m = 1, \ldots, M; n = 0, \ldots, N)$$
$$\hat{w}_i = \hat{W}_i^{mn}\sin\alpha_m x\cos\beta_n y \tag{12}$$
$$(m = 1, \ldots, M; n = 0, \ldots, N)$$

where $\alpha_m = \pi m/L$, $\beta_n = n/R$, m and n being the numbers of axial half waves and circumferential waves, respectively, and U_i^{mn}, V_i^{mn}, and W_i^{mn} are coefficients to be determined. It is noted that the solution form (11) is chosen so as to satisfy identically the linear part of the governing equations (9). In addition, by means of Eqs. (12), the radial shell imperfection $\hat{w}_i$ is expanded in the same form as the radial displacement w_i.

Substituting Eqs. (11) and (12) into the governing equations (9), and performing the integrations over the shell mean surface, the following set of nonlinear algebraic equations is obtained:

δU_i^{mn}:

$$
\begin{aligned}
&A_n\Big[(\alpha_m^2 D_{11}^{ij} + \beta_n^2 D_{66}^{ij} + \bar{\bar{D}}_{55}^{ij}) U_j^{mn} - \alpha_m\beta_n (D_{12}^{ij} + D_{66}^{ij}) V_j^{mn} \\
&\quad - \alpha_m \Big(\frac{1}{R} D_{12}^{ij} + \bar{D}_{13}^{ij} - \bar{D}_{55}^{ji} \Big) W_j^{mn} \Big] \\
&\quad + (- \alpha_m \alpha_r \alpha_p D_{11}^{ijk} L_{mrp}^{scc} C_{nsq}^{ccc} - \alpha_m \beta_s \beta_q D_{12}^{ijk} L_{mrp}^{sss} C_{nsq}^{css} \\
&\quad + \beta_n \beta_s \alpha_p D_{66}^{ijk} L_{mrp}^{csc} C_{nsq}^{ssc} \\
&\quad + \beta_n \alpha_r \beta_q D_{66}^{ijk} L_{mrp}^{ccs} C_{nsq}^{scs}) (\tfrac{1}{2} W_k^{pq} + \hat{W}_k^{pq}) W_j^{rs} = Q_i^{mn}
\end{aligned} \tag{13a}
$$

δV_i^{mn}:

$$
\begin{aligned}
&A_n\Big\{ - \alpha_m\beta_n (D_{12}^{ij} + D_{66}^{ij}) U_i^{mn} + \Big[\alpha_m^2 D_{66}^{ij} + \beta_n^2 D_{22}^{ij} + \bar{\bar{D}}_{44}^{ij} \\
&\quad - \frac{1}{R} (\bar{D}_{44}^{ij} + \bar{D}_{44}^{ji}) + \frac{1}{R^2} D_{44}^{ij} \Big] V_j^{mn} + \beta_n \Big(\frac{1}{R} D_{22}^{ij} + \bar{D}_{23}^{ij} \\
&\quad + \frac{1}{R} D_{44}^{ij} - \bar{D}_{44}^{ij} \Big) W_j^{mn} \Big\} + (\beta_n \alpha_r \alpha_p D_{12}^{ijk} L_{mrp}^{scc} C_{nsq}^{ccc} \\
&\quad + \beta_n \beta_s \beta_q D_{22}^{ijk} L_{mrp}^{sss} C_{nsq}^{css} - \alpha_m \beta_s \alpha_p D_{66}^{ijk} L_{mrp}^{csc} C_{nsq}^{ssc} \\
&\quad - \alpha_m \alpha_r \beta_q D_{66}^{ijk} L_{mrp}^{ccs} C_{nsq}^{scs}) \Big(\tfrac{1}{2} W_k^{pq} + \hat{W}_k^{pq} \Big) W_j^{rs} = 0
\end{aligned} \tag{13b}
$$

δW_i^{mn}:

$$
\begin{aligned}
&A_n\Big[- \alpha_m \Big(\frac{1}{R} D_{12}^{ij} + \bar{D}_{13}^{ji} - \bar{D}_{55}^{ij} \Big) U_j^{mn} + \beta_n \Big(\frac{1}{R} D_{22}^{ij} + \bar{D}_{23}^{ji} \\
&\quad + \frac{1}{R} D_{44}^{ij} - \bar{D}_{44}^{ij} \Big) V_j^{mn} + \Big(D_{55}^{ji} \alpha_m^2 + D_{44}^{ji} \beta_n^2 + \frac{1}{R^2} D_{22}^{ij} \\
&\quad + \frac{1}{R} \bar{D}_{23}^{ij} + \frac{1}{R} \bar{D}_{23}^{ji} + \bar{\bar{D}}_{33}^{ij} \Big) W_j^{mn} \Big] + (- \alpha_m \alpha_r \alpha_p D_{11}^{ijk} L_{mrp}^{csc} C_{nsq}^{ccc} \\
&\quad - \beta_n \alpha_r \beta_q D_{12}^{ijk} L_{mrp}^{sss} C_{nsq}^{scs} + \beta_n \beta_s \alpha_p D_{66}^{ijk} L_{mrp}^{scc} C_{nsq}^{ssc} \\
&\quad + \alpha_m \beta_s \beta_q D_{66}^{ijk} L_{mrp}^{ccs} C_{nsq}^{css}) (W_k^{pq} + \hat{W}_k^{pq}) U_j^{rs} \\
&\quad + (\alpha_m \beta_s \alpha_p D_{12}^{ijk} L_{mrp}^{csc} C_{nsq}^{ccc} + \beta_n \beta_s \beta_q D_{22}^{ijk} L_{mrp}^{sss} C_{nsq}^{scs} \\
&\quad - \beta_n \alpha_r \alpha_p D_{66}^{ijk} L_{mrp}^{scc} C_{nsq}^{ssc} - \alpha_m \alpha_r \beta_q D_{66}^{ijk} L_{mrp}^{ccs} C_{nsq}^{css}) \\
&\quad \times (W_k^{pq} + \hat{W}_k^{pq}) V_j^{rs} + \Big[\alpha_r \alpha_p \Big(\frac{1}{R} D_{12}^{ijk} + \bar{D}_{13}^{jki} \Big) L_{mrp}^{scc} C_{nsq}^{ccc} \\
&\quad + \beta_s \beta_q \Big(\frac{1}{R} D_{22}^{ijk} + \bar{D}_{23}^{jki} \Big) L_{mrp}^{sss} C_{nsq}^{css} \Big] (\tfrac{1}{2} W_k^{pq} + \hat{W}_k^{pq}) W_j^{rs} \\
&\quad + \Big[\alpha_m \alpha_p \Big(\frac{1}{R} D_{22}^{ijk} + \bar{D}_{13}^{ikj} \Big) L_{mrp}^{csc} C_{nsq}^{ccc} + \beta_n \beta_q \Big(\frac{1}{R} D_{22}^{ijk} \\
&\quad + \bar{D}_{23}^{ikj} \Big) L_{mrp}^{sss} C_{nsq}^{scs} \Big] (W_k^{pq} + \hat{W}_k^{pq}) W_j^{rs} \\
&\quad + (\alpha_m \alpha_r \alpha_p \alpha_g D_{11}^{ijkl} L_{mrpg}^{cccc} C_{nsqh}^{cccc} \\
&\quad + \alpha_m \beta_s \alpha_p \beta_h D_{12}^{ijkl} L_{mrpg}^{cscs} C_{nsqh}^{cscs} + \beta_n \alpha_r \beta_q \alpha_g D_{12}^{ijkl} L_{mrpg}^{scsc} C_{nsqh}^{scsc} \\
&\quad + \beta_n \beta_s \beta_q \beta_h D_{22}^{ijkl} L_{mrpg}^{ssss} C_{nsqh}^{ssss} + \alpha_m \alpha_r \beta_q \beta_h D_{66}^{ijkl} L_{mrpg}^{ccss} C_{nsqh}^{ccss} \\
&\quad + \alpha_m \beta_s \beta_q \alpha_g D_{66}^{ijkl} L_{mrpg}^{cssc} C_{nsqh}^{cssc} + \beta_n \alpha_r \alpha_p \beta_h D_{66}^{ijkl} L_{mrpg}^{sccs} C_{nsqh}^{sccs} \\
&\quad + \beta_n \beta_s \alpha_p \alpha_g D_{66}^{ijkl} L_{mrpg}^{sscc} C_{nsqh}^{sscc}) (\tfrac{1}{2} W_k^{pq} + \hat{W}_k^{pq}) \\
&\quad \times (W_l^{gh} + \hat{W}_l^{gh}) W_j^{rs} = P_i^{mn}
\end{aligned} \tag{13c}
$$

where the load terms are defined as follows:

$$
P_1^{mn} = \begin{cases} 0, & n \neq 0 \\ 0, & n = 0, \quad m \quad \text{even} \\ p_b 4LR/m, & n = 0, \quad m \quad \text{odd} \end{cases}
$$

$$
P_{N+1}^{mn} = \begin{cases} 0, & n \neq 0 \\ 0, & n = 0, \quad m \quad \text{even} \\ -p_t 4LR/m, & n = 0, \quad m \quad \text{odd} \end{cases} \tag{14}
$$

$$
Q_i^{mn} = q_0 \begin{cases} 0, & n \neq 0 \\ 2\pi R(t_i + t_{i-1}) \quad \text{at the } i\text{th node}, & n = 0 \\ 2\pi R t_1 \quad \text{at node 1}, & n = 0 \\ 2\pi R t_N \quad \text{at node } N+1, & n = 0 \end{cases}
$$

Moreover,

$$
\begin{aligned}
L_{ij\cdots}^{sc\cdots} &\equiv \int_0^L \sin \alpha_i x \cos \alpha_j x \ldots \, dx \\
C_{ij\cdots}^{sc\cdots} &\equiv \int_0^{2\pi R} \sin \beta_i y \cos \beta_j y \ldots \, dy
\end{aligned} \tag{15a}
$$

$$
A_n = \begin{cases} \dfrac{L\pi R}{2} & \text{for} \quad n \neq 0 \\ L\pi R & \text{for} \quad n = 0 \end{cases} \tag{15b}
$$

The integral coefficients L and C defined in Eqs. (15a) are obtained by the integration of products of trigonometric functions over the length and circumferential coordinates, respectively. The nonzero coefficients are listed in Appendix 2 of Reddy and Savoia.[35]

IV. Numerical Results

A. Buckling Analysis

It is usual to perform a linearized buckling analysis before the full nonlinear analysis in order to select those modes that dominate the prebuckling and buckling behavior of the shell. In fact, this criterion can be profitably used to select the modes to be included in the displacement expansion (1), so reducing the required core size and the time required for obtaining the numerical solution.

In this context, the following prebuckling stress state is assumed[28] to be that corresponding to a pure membrane state where the end effects are disregarded:

$$
\sigma_1 = -q_0, \qquad \sigma_2 = (p_b + p_t)R/h, \qquad \sigma_3 = \sigma_4 = \sigma_5 = \sigma_6 = 0 \tag{16}
$$

Consequently, the second-order work of the prebuckling stresses can be written as

$$
\delta W = \int_0^L \int_0^{2\pi R} \Big(M_1^{ij} \frac{\partial \delta w_i}{\partial x} \frac{\partial w_j}{\partial x} + M_2^{ij} \frac{\partial \delta w_i}{\partial y} \frac{\partial w_j}{\partial y} \Big) \, dx \, dy \tag{17}
$$

with

$$M_1^{ij} = -q_0 I^{ij}, \qquad M_2^{ij} = (p_b + p_t)RI^{ij}/h \tag{18a}$$

$$I^{ij} = \int_{-h/2}^{h/2} \Phi^i \Phi^j \, dz \tag{18b}$$

Making use of the displacement expansion (1), the following eigenvalue problem is obtained for any mode (m,n):

$$\left(\begin{bmatrix} [S_{11}] & [S_{12}] & [S_{13}] \\ [S_{12}]^T & [S_{22}] & [S_{23}] \\ [S_{13}]^T & [S_{23}]^T & [S_{33}] \end{bmatrix} - q_0 \begin{bmatrix} [0] & [0] & [0] \\ [0] & [0] & [0] \\ [0] & [0] & [M_{33}] \end{bmatrix} \right) \begin{Bmatrix} \{U^{mn}\} \\ \{V^{mn}\} \\ \{W^{mn}\} \end{Bmatrix} = \begin{Bmatrix} \{0\} \\ \{0\} \\ \{0\} \end{Bmatrix} \tag{19}$$

where $S_{\alpha\beta}^{ij}(i,j = 1, 2, \ldots, N+1; \alpha,\beta = 1, 2, 3)$ are the linear coefficients of Eqs. (13) (see Ref. 35), and $M_{33}^{ij} = \alpha_m^2 I^{ij}$.

In order to bring out the notable differences between the buckling response of isotropic and multilayered cylinders, a buckling analysis has been carried out. Four cases of thin ($h = 0.254$ cm) and thick ($h = 7.62$ cm) isotropic and multilayered shells with $R = 91.4$ cm and $L = 254$ cm are considered. The elastic properties used are given in the following.

Isotropic shell:

$$E = 209.5 \text{ GPa } (30 \times 10^6 \text{ psi}), \quad \nu = 0.3 \tag{20a}$$

Three-layered cross ply (0 deg/90 deg/0 deg) shell:

$$\begin{aligned} E_L &= 209.5 \text{ GPa } (30 \times 10^6 \text{ psi}), \qquad E_T = 7 \text{ GPa } (10^6 \text{ psi}) \\ G_{LT} &= 3.5 \text{ GPa } (0.5 \times 10^6 \text{ psi}) \\ G_{TT} &= 1.4 \text{ GPa } (0.2 \times 10^6 \text{ psi}) \\ \nu_{LT} &= \nu_{TT} = 0.3, \qquad h_i = h/3 \end{aligned} \tag{20b}$$

where subscripts L and T stand for directions along and transverse to the fibers, respectively.

Figure 2 depicts the plots of ratios of buckling load over the minimum buckling load (q_b/q_{mb}) for different values of the half axial wave number m and the circumferential wave number n. For isotropic cylinders, the minimum buckling load agrees very well with the well-known classical buckling load[34]:

$$q_{cl} = \frac{Eh}{R\sqrt{3(1-\nu^2)}} \tag{21}$$

For the thin isotropic cylinder (Fig. 2a), the level lines of the eigenvalue map are very similar to the Koiter's circles[6] for infinitely long thin isotropic cylinders; Koiter[6] pointed out that only for high wave numbers the effect of restrained ends has some influence on buckling loads. In addition, it is noted that there are many modes whose eigenvalues are only slightly higher than the lowest eigenvalue ($q_b/q_{mb} \simeq 1$): for thin shell geometry 119 modes (located in the area marked with dots in the eigenvalue map) exhibit a buckling load about 10% higher than the minimum buckling load. Hence, in this case, there is no way to find the actual postbuckling path, i.e., the exact number of waves in which the shell buckles. To obtain some reasonable results, an accurate analysis of the amplitude of the

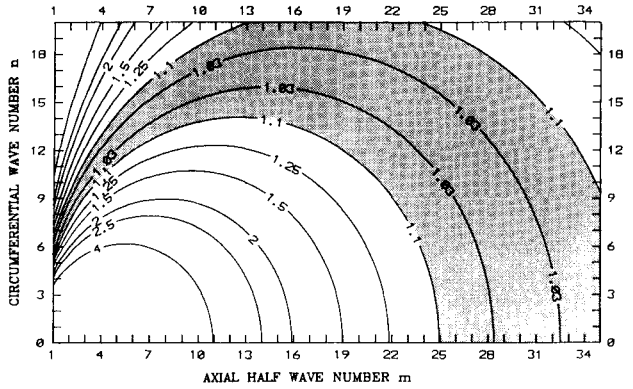

a) Thin isotropic cylinder: $L = 254$ cm; $R = 91.4$ cm; $h = 0.254$ cm

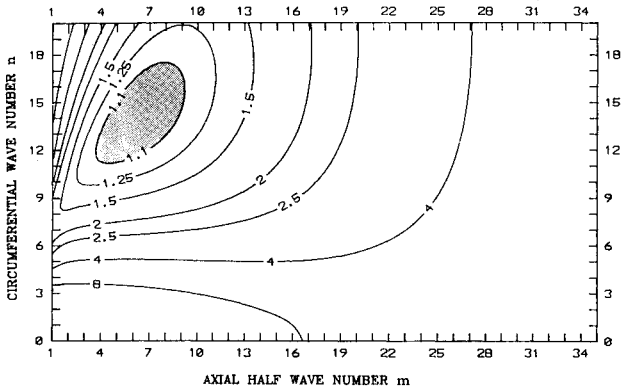

b) Thick isotropic cylinder: $L = 254$ cm; $R = 91.4$ cm; $h = 7.62$ cm

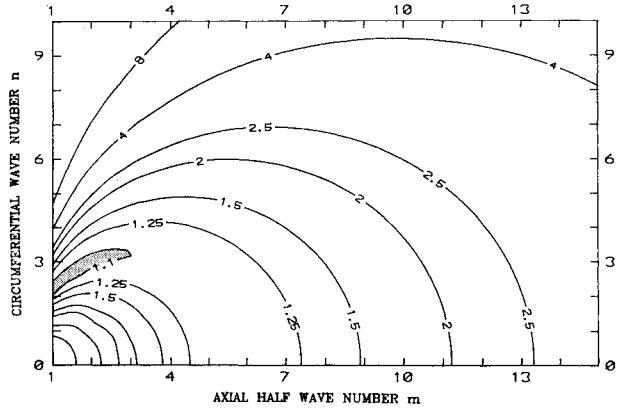

c) Thin three-layered cylinder: $L = 254$ cm; $R = 91.4$ cm; $h = 0.254$ cm

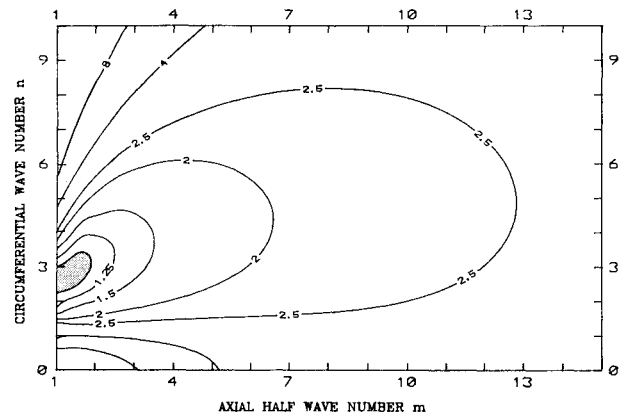

d) Thick three-layered cylinder: $L = 254$ cm; $R = 91.4$ cm; $h = 7.62$ cm

Fig. 2 Linearized buckling analysis: the modes included in the areas marked by dots have an eigenvalue ratio less than 1.1.

initial geometry imperfection, based on experimental data, is needed,[32,36] and a multimode approach may require an enormous number of modes. For these reasons, two- or three-mode analyses,[3,4] even though they are very important to understand the erosion mechanism of the membrane stiffness in the postbuckling path, cannot be used to achieve good estimates of the maximum load and imperfection sensitivity.

When the wall thickness is increased to $h = 7.62$ cm (Fig. 2b), the overall behavior is not changed from the previous case, but now the lowest buckling load is single valued, and only two other modes show a ratio q_b/q_{mb} less than 1.1. Unlike in the thin shell case because of the high bending rigidity of the thick shell, these modes are associated with only one or two half waves in the axial direction.

For multilayered thin (Fig. 2c) and thick (Fig. 2d) fiber-reinforced cylinders, the behavior is substantially different from the isotropic one. For both cases, the maps of buckling loads suggest that very few modes are required in a nonlinear multimode analysis.

B. Postbuckling Analysis

Examples of postbuckling behavior of imperfect multilayered cylindrical shells are presented here for different values of the wall imperfection. The imperfection is represented in terms of an increment to the radial deflection, and the increment $\hat{w}$ is assumed to be in the same form as the displacement field [see e.g., Eqs. (1)]. The nonlinear equations (13) are solved making use of the Riks-Wempner incremental iterative scheme[37-39] in order to follow the equilibrium path even through limit points. The tangent stiffness matrix is presented in Appendix 3 of Reddy and Savoia.[35]

Two example problems are considered here, namely, three-layered thin ($h = 0.254$ cm) and moderately thick ($h = 2.54$ cm) shells with $R = 91.4$ cm, $L = 254$ cm, and elastic properties presented in Eq. (20b).

Figures 3 show plots of the axial load vs the axial deflection for three different amplitudes of the initial imperfections. The axial load is normalized with respect to the minimum buckling load obtained from the linear eigenvalue analysis. For the thin shell case (Fig. 3a), the unstable postbuckling behavior is related to the coupling between the modes (6,13), (6,14), and (6,15). The maximum load obtained is approximately one half of the buckling load predicted by the eigenvalue analysis, whereas the minimum postbuckling load is 0.38 times the critical buckling load. In accordance with Pedersen,[2,9] the maximum load can be reached only for shells with very small imperfections. For higher imperfections (shown by dashed lines in Fig. 3a), a gradual transition from the pure membrane prebuckling behavior to the nonlinear response occurs. In the same figure, the deformed shape in the postbuckling path is included.

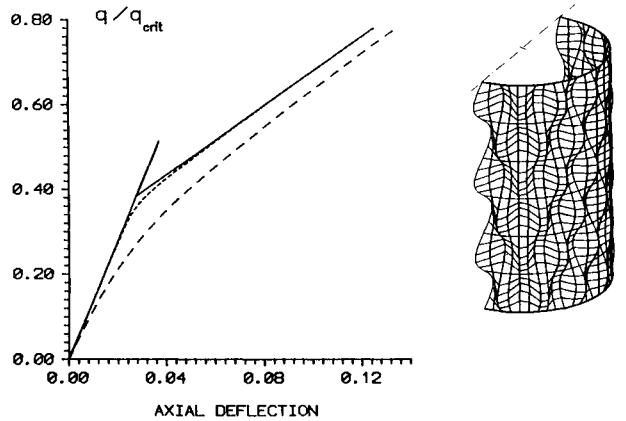

Fig. 3a Postbuckling analysis: load vs normalized axial deflection U/h (at $x = L$, $y = 0$, $z = -h/2$) equilibrium path for a thin three-layered cylinder ($L = 254$ cm, $R = 91.4$ cm, $h = 0.254$ cm) for different values of the mode imperfections: ——$\hat{W}^i_{mn} = -10^{-6}$; · · · · $\hat{W}^i_{mn} = -10^{-3}$; ----$\hat{W}^i_{mn} = -10^{-2}$.

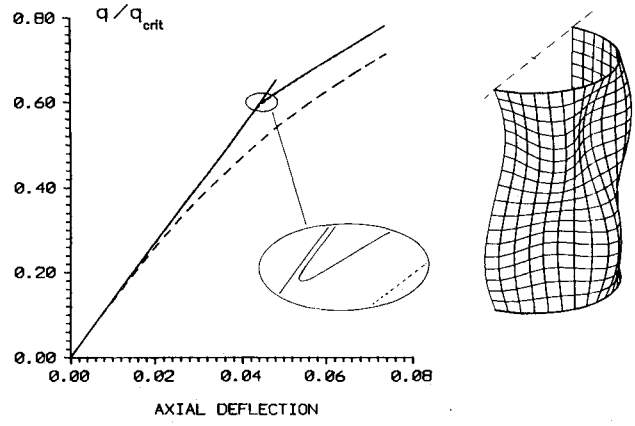

Fig. 3b Postbuckling analysis: load vs normalized axial deflection U/h (at $x = L$, $y = 0$, $z = -h/2$) equilibrium path for a moderately thick three-layered cylinder ($L = 254$ cm, $R = 91.4$ cm, $h = 2.54$ cm) for different values of the mode imperfections: ——$\hat{W}^i_{mn} = -10^{-5}$; · · · · $\hat{W}^i_{mn} = -10^{-3}$; ----$\hat{W}^i_{mn} = -10^{-1}$.

The postbuckling response for the moderately thick shell is presented in Fig. 3b. In this case, the unstable behavior is related to coupling of modes (2,4) and (2,5), as it is also shown by the deformed shape reported. The thick cylinder shows a postbuckling branch stiffer than the thin cylinder because of its higher bending rigidity. The particulars of the transition at the minimum postbuckling load is highlighted in Fig. 3b.

V. Conclusions

The postbuckling response of circular cylindrical shells made of cross-ply lamination schemes is studied using the layer-wise shell theory. The effect of imperfection on the postbuckling response is investigated for isotropic and cross-ply and thin and thick cylindrical shells with simply supported boundary conditions. Thin isotropic cylinders exhibit many eigenvalues close to the minimum eigenvalue. For thick cylinders, the number of eigenvalues close to the minimum eigenvalue is relatively small. On the other hand, cross-ply composite cylindrical shells, thin or thick, show less number of eigenvalues closer to the minimum eigenvalues. When the cylinder is thick, the number is further reduced.

In the postbuckling analysis, it is observed that the magnitude of imperfection has an effect on the load-carrying capacity of the shells. The maximum load-carrying capacity of a shell can be achieved only for small imperfection (say, $10^{-5} \sim 10^{-4}$ times the thickness of the shell). For large imperfections, the shell does not exhibit any obvious elastic limit load; the nonlinear load-deflection curves indicate softening structural response. In the postbuckling regime, thick cylinders show higher stiffness when compared to thin cylinders. This is due to the large bending rigidity of thick shells.

Acknowledgments

The support of this work by NAG-1-1085 from NASA Langley Research Center is gratefully acknowledged. The second author was supported by the Italian Ministry of University and Scientific and Technological Research and the National Council of Research. The first author wishes to acknowledge the support and encouragement by John Dalessandros of General Dynamics (Space Systems Division).

References

[1]Hutchinson, J. W., and Koiter, W. T., "Postbuckling Theory," *Journal of Applied Mechanics,* Vol. 23, No. 12, 1970, pp. 1353-1366.

[2]Pedersen, P. T., "On the Collapse Load of Cylindrical Shells," *Buckling of Structures,* edited by B. Budiansky, Springer-Verlag, Berlin, 1974, pp. 27-39.

[3]Croll, J. G. A., and Batista, R. C., "Explicit Lower Bounds for the Buckling of Axially Loaded Cylinders," *International Journal of Mechanical Sciences,* Vol. 23, No. 6, 1981, pp. 331-343.

[4]Hunt, G. W., Williams, K. A. J., and Cowell, R. G., "Hidden Symmetry Concepts in the Elastic Buckling of Axially-Loaded Cylinders," *International Journal of Solids and Structures,* Vol. 22, No. 12, 1986, pp. 1501–1515.

[5]Simitses, G. J., "Buckling and Postbuckling of Imperfect Cylindrical Shells: A Review," *Applied Mechanics Review,* Vol. 39, No. 10, 1986, pp. 1517–1524.

[6]Koiter, W. T., "Over de stabiliteit van net alestisch evenwicht," Thesis, Delft, H. J. Paris, Amsterdam; also English Translation, "On the Stability of Elastic Equilibrium," NASA TT-F10833, 1967.

[7]Semenyuk, N. P., and Zhukova, N. B., "Initial Post-Critical Behaviour of Layered Cylindrical Shells of Composites," *Mekhanika Kompozituykh Materialov,* Vol. 23, No. 1, 1987, pp. 88–93; also, (in English), *Mechanics Composite Materials,* Vol. 23, No. 1, pp. 78–83.

[8]Pandey, M. D., and Sherbourne, A. N., "Imperfection Sensitivity of Optimized Laminated Composite Shells: A Physical Approach," *International Journal of Solids and Structures,* Vol. 27, No. 12, 1991, pp. 1575–1595.

[9]Pedersen, P. T., "Buckling of Unstiffened and Ring Stiffened Cylindrical Shells Under Axial Compression,"*International Journal of Solids and Structures,* Vol. 9, No. 5, 1973, pp. 671–691.

[10]Donnell, L. H., "A New Theory for the Buckling Analysis of Thin Cylinders Under Axial Compression and Bending," *Transactions of the American Society of Mechanical Engineers,* Vol. 56, 1934, pp. 795–806.

[11]Von Kármán, TH., and Tsien, H. S., "The Buckling of Thin Cylindrical Shells Under Axial Pressure," *Journal of Aeronautical Sciences,* Vol. 8, No. 8, 1941, pp. 303–312.

[12]Almroth, B. O., "Postbuckling Behavior of Axially Compressed Circular Cylinders," *AIAA Journal,* Vol. 1, No. 3, 1963, pp. 630–633.

[13]Hoff, N. J., Masden, W. A., and Mayers, J., "Postbuckling Equilibrium of Axially Compressed Circular Cylinders Shells," *AIAA Journal,* Vol. 4, No. 1, 1966, pp. 126–133.

[14]Tasi, J., "Effect of Heterogeneity on the Stability of Composite Cylindrical Shells Under Axial Compression," *AIAA Journal,* Vol. 4, No. 6, 1965, pp. 1058–1062.

[15]Khot, N. S., "Buckling and Postbuckling Behavior of Composite Cylindrical Shells Under Axial Compression," *AIAA Journal,* Vol. 8, No. 2, 1970, pp. 229–235.

[16]Hoff, N. J., "The Perplexing Behavior of Thin Cylindrical Shells in Axial Compression," *Israel Journal of Technology,* Vol. 4, No. 1, 1966, pp. 1–28.

[17]Esslinger, M., and Geier, B., *Post-Buckling Behaviour of Structures,* Springer-Verlag, Vienna, 1975.

[18]Bushnell, D., *Computerized Buckling of Shells,* Martinus Nijhoff, Kluver Acad., Norwell ME, 1985.

[19]Singer, J., and Rosen, A., "The Influence of Boundary Conditions on the Buckling of Stiffened Cylindrical Shells," *Buckling of Structures,* edited by B. Budiansky, Springer-Verlag, Berlin, 1974, pp. 227–250.

[20]Narasimhan, K. Y., and Hoff, N. J., "Snapping of Imperfect Thin-Walled Circular Cylindrical Shells of Finite Length," *Journal of Applied Mechanics,* Vol. 38, No. 1, 1971, pp. 162–171.

[21]Arbocz, J., and Sechler, E. E., "On the Buckling of Axially Compressed Imperfect Cylindrical Shells," *Journal of Applied Mechanics,* Vol. 41, No. 3, 1974, pp. 737–743.

[22]Iu, V. P., and Chia, C. Y., "Effect of Transverse Shear on Nonlinear Vibration and Post-Buckling of Antisymmetric Cross-Ply Imperfect Cylindrical Shells," *International Journal of Solids and Structures,* Vol. 29, No. 2, 1988, pp. 195–210.

[23]Tennyson, R. C., and Chan, K. C., "Buckling of Imperfect Sandwich Cylinders Under Axial Compression," *International Journal of Solids and Structures,* Vol. 26, No. 9/10, 1990, pp. 1017–1036.

[24]Reddy, J. N., "On Refined Computational Models of Composite Laminates," *International Journal for Numerical Methods in Engineering,* Vol. 27, No. 2, 1989, pp. 361–382.

[25]Savoia, M., and Reddy, J. N., "A Variational Approach to Three-Dimensional Elasticity Solutions of Laminated Composite Plates," *Journal of Applied Mechanics* (to be published).

[26]Reddy, J. N., "A Generalization of Two-Dimensional Theories of Laminated Composite Plates," *Communications in Applied Numerical Methods,* Vol. 3, No. 3, 1987, pp. 173–180.

[27]Barbero, E. J., and Reddy, J. N., "General Two-Dimensional Theory of Laminated Cylindrical Shells," *AIAA Journal,* Vol. 28, No. 3, 1990, pp. 544–553.

[28]Reddy, J. N., "A Layer-Wise Shell Theory with Applications to Buckling and Vibration of Cross-Ply Laminated Stiffened Circular Cylindrical Shells," Center for Composite Materials and Structures, Rept. CCMS-92-01, Virginia Polytechnic Inst. and State Univ., Blacksburg, VA, Jan. 1992.

[29]Robbins, D. H., and Reddy, J. N., "On the Modeling of Thick Composites Using a Layer-Wise Theory," *International Journal for Numerical Methods in Engineering* (to be published).

[30]Khot, N. S., Venkayya, V. B., and Berke, L., "Buckling and Postbuckling of Initially Imperfect Orthotropic Cylindrical Shells Under Axial Compression and Internal Pressure," *Instability of Continuous Systems,* edited by H. Leipholz, Springer-Verlag, Berlin, 1971, pp. 392–398.

[31]Simitses, G. J., Shaw, D., and Sheinman, I., "Stability of Cylindrical Shells by Various Nonlinear Shell Theories," *Zeitschrift für Angewandte Mathematik und Mechanic,* Vol. 65, No. 1, 1985, pp. 159–166.

[32]Arbocz, J., and Babcock, C. D., "Prediction of Buckling Loads Based on Experimentally Measured Initial Imperfections," *Buckling of Structures,* edited by B. Budiansky, Springer-Verlag, Berlin, 1974, pp. 291–311.

[33]Arbocz, J., "Post-Buckling Behaviour of Structures—Numerical Techniques for More Complicated Structures," *Buckling and Post-Buckling, Lecture Notes in Physics,* Springer-Verlag, Berlin, 1987, pp. 84–142.

[34]Donnell, L. H., *Beams, Plates and Shells,* McGraw-Hill, New York, 1976.

[35]Reddy, J. N., and Savoia, M., "Postbuckling of Laminated Circular Cylindrical Shells According to the Layer-Wise Shell Theory," Center for Composite Materials and Structures Rept. CCMS-92-02, Virginia Polytechnic Inst. and State Univ., Blacksburg, VA, Jan. 1992.

[36]Sheinman, I., and Simitses, G. J., "Buckling Analysis of Geometrically Imperfect Stiffened Cylinders Under Axial Compression," *AIAA Journal,* Vol. 15, No. 3, 1977, pp. 374–382.

[37]Wempner, G. A., "Discrete Approximations Related to Nonlinear Theories of Solids," *International Journal of Solids and Structures,* Vol. 7, No. 11, 1971, pp. 1581–1599.

[38]Riks, E., "An Incremental Approach to the Solution of Snapping and Buckling Problems," *International Journal of Solids and Structures,* Vol. 15, No. 7, 1979, pp. 529–551.

[39]Crisfield, M. A., "A Fast Incremental/Iterative Solution Procedure that Handles 'Snap-Through,' " *Computers and Structures,* Vol. 13, No. 1–3, 1981, pp. 55–62.